Strong and radiative decays of the scalars $f_0(980)$ and $a_0(980)$ in a hadronic molecule approach

Tanja Branz, Thomas Gutsche, and Valery E. Lyubovitskij*

Institut für Theoretische Physik, Universität Tübingen, Auf der Morgenstelle 14, D-72076 Tübingen, Germany

(Received 7 August 2008; published 3 December 2008)

We analyze the electromagnetic and strong decay properties of the light scalars $a_0(980)$ and $f_0(980)$ within a hadronic molecule interpretation. Both scalars are discussed within a covariant and gauge invariant model which also allows for finite size effects due to their spatially extended structure in the $K\bar{K}$-bound state picture. Allowing for f_0-a_0 mixing we also study its influence on the radiative decays $f_0/a_0 \to \gamma\gamma$, $f_0/a_0 \to \gamma\omega$, and $f_0/a_0 \to \gamma\rho$ as well as the ϕ production of the f_0 and a_0. Furthermore, we apply our formalism to describe the strong $f_0 \to \pi\pi$ and $a_0 \to \pi\eta$ decay properties.

DOI: 10.1103/PhysRevD.78.114004 PACS numbers: 13.25.Jx, 13.40.Hq, 36.10.Gv

I. INTRODUCTION

Until now meson spectroscopy provides a valuable tool to explore the structure and properties of mesons and, extending the scope, to get further information on the confinement regime of strong interaction. During the last decade the meson mass spectrum showed a richer structure than might be expected from the constituent quark model, which decisively influenced our understanding of hadronic structure in the past. In particular, the structure issue of the lightest scalars has been under permanent discussion concerning mesonic structure beyond the quark-antiquark picture. There exist different approaches concerning the substructure of the $f_0(980)$ and its ''twin'', the $a_0(980)$, which range from $q\bar{q}$ [1–3] to tetraquark $q^2\bar{q}^2$ [4–6] interpretations. In [7] the structure of the light scalar nonet including $f_0(980)$ was tested using radiative ϕ decays. The authors of Ref. [7] point out the difficulty to distinguish between the $q\bar{q}$ and the $qq\bar{q}\,\bar{q}$ picture for the light scalar mesons. A possible admixture between $\bar{q}q$ and $qq\bar{q}\,\bar{q}$ configurations for the low-lying scalar mesons has been considered in Ref. [8] using the chiral approach. Both scalars are also discussed in a clustered version of the tetraquark configuration where the two quarks and antiquarks form a bound state of mesons—hadronic molecules [9–11]. In addition, an isospin-violating mixture of the $f_0(980)$ and $a_0(980)$ mesons has been originally discussed in [12] and taken into consideration in [13–15] which provides an interesting possibility to study its substructure. f_0-a_0 mixing is on the one hand motivated by their near degenerate masses, on the other hand by the mass gap between the nearby charged and neutral $K\bar{K}$ thresholds. A crucial check for theoretical considerations will be future experiments planning to investigate f_0-a_0 mixing (see e.g. Ref. [16]).

In the present paper we study the electromagnetic and strong decay properties of the $f_0(980)$ and $a_0(980)$ mesons which are assumed to be of a pure molecular meson structure, that is bound states of two kaons. We discuss the electromagnetic decays with the final states occupied by photons and massive vector mesons $S \to V\gamma$, $S \to \gamma\gamma$, and $\phi \to S\gamma$, where $S = f_0$, a_0, and $V = \rho$, ω, as well as the strong $a_0/f_0 \to \pi\pi/\pi\eta$ decay properties.

For the description of the $f_0(980)$ and $a_0(980)$ as hadronic molecules we apply the theoretical framework developed in [17] based on the use of the compositeness condition $Z = 0$ [18,19] which implies that the renormalization constant of the hadron wave function is set equal to zero. Note that this condition was originally applied to the study of the deuteron as a bound state of the proton and neutron [18]. Then it was extensively used in the low-energy hadron phenomenology as the master equation for the treatment of mesons and baryons as bound states of light and heavy constituent quarks (see Refs. [19,20]). In Refs. [21] the compositeness condition has been successfully used in the description of the recently discovered heavy mesons as hadronic molecules. In particular, within the mesonic bound state interpretation, the compositeness condition allows for a self-consistent determination of the coupling of the scalar mesons to their constituents. The advantage of our approach is that it has a clear and consistent mathematical structure with a minimal amount of free parameters. It also fulfills essential conditions such as covariance and gauge invariance, while allowing to include the spatially extended structure of the meson molecules and isospin-violating mixing effects. Here we generate the f_0-a_0 mixing due to the mass difference of intermediate charged and neutral kaon loops; this mechanism was proposed in [12] as the leading contribution to the f_0-a_0 mixing. Note that in our approach this mixing mechanism is naturally generated due to the coupling of a_0 and f_0 to its constituents—the kaons.

The paper is organized as follows. Our framework is discussed in Sec. II. We derive the effective mesonic Lagrangian for the treatment of f_0 and a_0 as $K\bar{K}$ bound states (molecules) in Sec. II A. In Sec. II B we discuss the modification of $f_0K\bar{K}$ and $a_0K\bar{K}$ couplings due to the f_0-a_0 mixing. In Sec. II C we include the electromagnetic interactions and discuss the diagrams contributing to the

*On leave of absence from the Department of Physics, Tomsk State University, 634050 Tomsk, Russia.

radiative decays of f_0 and a_0. Our results are presented in Sec. III, which we also compare with other approaches and with experimental data. In Sec. IV we present a short summary of our results.

II. THEORETICAL FRAMEWORK

A. Molecular structure of the $f_0(980)$ and $a_0(980)$ mesons

The theoretical framework we use for our analysis is based on the nonlocal strong Lagrangians [17,20–23]

$$\mathcal{L}_{f_0K\bar{K}} = \frac{g_{f_0K\bar{K}}}{\sqrt{2}} f_0(x) \int dy \Phi(y^2) \bar{K}\left(x - \frac{y}{2}\right) K\left(x + \frac{y}{2}\right),$$
$$\mathcal{L}_{a_0K\bar{K}} = \frac{g_{a_0K\bar{K}}}{\sqrt{2}} \vec{a}_0(x) \int dy \Phi(y^2) \bar{K}\left(x - \frac{y}{2}\right) \vec{\tau} K\left(x + \frac{y}{2}\right), \tag{1}$$

describing the interaction between the kaon-antikaon bound state and its constituents. The kaon and scalar fields are collected in the kaon isospin doublets and the scalar meson triplet

$$K = \begin{pmatrix} K^+ \\ K^0 \end{pmatrix}, \qquad \bar{K} = \begin{pmatrix} K^- \\ \bar{K}^0 \end{pmatrix}, \quad \text{and} \quad \vec{a}_0 = (a_0^+, a_0^0, a_0^-). \tag{2}$$

The vector $\vec{\tau} = (\tau^+, \tau^0, \tau^-)$ is characterized by the Pauli matrices $\tau_{i=1,2,3}$, where $\tau^{\pm} = \frac{1}{\sqrt{2}}(\tau_1 \pm i\tau_2)$ and $\tau^0 = \tau_3$.

Finite size effects are incorporated in our model by the correlation function $\Phi(y^2)$. Its Fourier transform $\tilde{\Phi}(k_E^2)$ is directly related to the shape and size of the hadronic molecule and shows up as the form factor in the Feynman diagrams. Here, we employ a Gaussian form

$$\Phi(y^2) = \int \frac{d^4k}{(2\pi)^4} \tilde{\Phi}(-k^2) e^{-iky}$$
$$\text{with } \tilde{\Phi}(k_E^2) = \exp(-k_E^2/\Lambda^2), \tag{3}$$

where the index E refers to the Euclidean momentum space. The size parameter Λ controls the spatial extension of the hadronic molecule and is varied around 1 GeV. In the special case of pointlike interaction, which we refer to as the local case, the correlation function $\Phi(y^2)$ is replaced by the delta function $\lim_{\Lambda\to\infty} \Phi(y^2) = \delta^{(4)}(y)$.

The couplings to the constituent kaons, $g_{SK\bar{K}}$ with $S = f_0, a_0$, are determined self-consistently within our model by using the compositeness condition. It provides a method to fix the coupling strength between a bound state and its constituents [18,19]; it therefore reduces the amount of free input parameters and also allows for a clear and straightforward determination of the decay properties. Note that this condition has also been used in the $K\bar{K}$ molecule approach in [10,24]. The coupling constant can be easily extracted from the definition of the field renormalization constant Z_{f_0} which is set to zero

$$Z_S = 1 - \tilde{\Pi}'(M_{f_0}^2) = 0. \tag{4}$$

Here, $\tilde{\Pi}'(M_{f_0}^2) = \frac{g_{f_0K\bar{K}}^2}{(4\pi)^2} \tilde{\Sigma}'(M_{f_0}^2)$ is the derivative of the mass operator

$$\Sigma(p^2) = \int \frac{d^4k}{\pi^2 i} \tilde{\Phi}^2(-k^2) S\left(k + \frac{p}{2}\right) S\left(k - \frac{p}{2}\right) \tag{5}$$

shown in Fig. 1. We stress that the Weinberg condition applies only to the bound states. In general, meson-loop diagrams are evaluated by using the free meson propagators given by

$$iS_K(x-y) = \langle 0|TK(x)K^\dagger(y)|0\rangle = \int \frac{d^4k}{(2\pi)^4 i} e^{-ik(x-y)} S_K(k), \tag{6}$$

in case of scalar and pseudoscalar mesons, where

$$S_K(k) = \frac{1}{M_K^2 - k^2 - i\epsilon}. \tag{7}$$

For vector and axial-vector fields ($H^* = V, A$) we use

$$iS_{H^*}^{\mu\nu}(x-y) = \langle 0|TH^{*\mu}(x)H^{*\nu\dagger}(y)|0\rangle = \int \frac{d^4k}{(2\pi)^4 i} e^{-ik(x-y)} S_{H^*}^{\mu\nu}(k) \tag{8}$$

with

$$S_{H^*}^{\mu\nu}(k) = \frac{-g^{\mu\nu} + k^\mu k^\nu / M_{H^*}^2}{M_{H^*}^2 - k^2 - i\epsilon}. \tag{9}$$

B. Inclusion of f_0-a_0 mixing

The isospin-violating mixture of the $f_0(980)$ and $a_0(980)$ mesons was originally discussed in [12] and also pursued later e.g. in Refs. [13–15]. In particular, in Ref. [12] a model-independent result for the f_0-a_0 mixing amplitude was derived due to the subtraction of charged and neutral kaon-loop diagrams, which is valid for any value of external momenta. In our approach this mixing amplitude (see Fig. 2) is naturally generated due to the coupling of f_0 and a_0 to their constituent kaons. In the following we restrict the calculation to this leading contribution of the f_0-a_0 mixing mechanism. The mixing effect leads to a renormalization of the f_0/a_0 couplings to the constituents. The modified $f_0K\bar{K}$ and $a_0K\bar{K}$ couplings are shown in Fig. 3(a) and 3(b). For the f_0 and a_0 propagators we use the ones in the Breit-Wigner form:

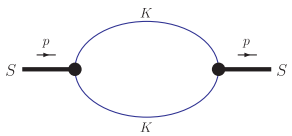

FIG. 1 (color online). Mass operator of $S = f_0, a_0$.

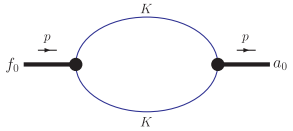

FIG. 2 (color online). Leading contribution to f_0-a_0 mixing.

$$D_S(p^2) = \frac{1}{M_S^2 - p^2 + iM_S\Gamma_S}, \tag{10}$$

where $\Gamma_S = \Gamma(M_S^2)$ is the total width of the $S = f_0(a_0)$ meson.

Note that the focus of the present considerations lie on the electromagnetic and strong scalar decay properties, where mixing modifies the coupling between the meson molecule and the $K\bar{K}$ constituents in the loop. In the following we show that this mixing effect is not so dramatic for isospin allowed transitions. However, for consistency we include such effects since the corresponding f_0-a_0 mixing insertions are naturally generated by our effective Lagrangian. We just stress that a more detailed theoretical analysis of the f_0-a_0 mixing effects was done in Refs. [12–15]. A direct access to the mixing strength can be obtained from isospin-violating processes, such as the $J/\psi \to \phi f_0 \to \phi a_0$ reaction, which is discussed in [16].

C. Inclusion of the electromagnetic interaction

The electromagnetic interaction terms are obtained by minimal substitution $\partial^\mu K^\pm \to (\partial^\mu \mp ieA^\mu)K^\pm$ in the free Lagrangian $\mathcal{L}_K$ of charged kaons

$$\mathcal{L}_K = \partial_\mu K^+ \partial^\mu K^- - M_K^2 K^+ K^- \tag{11}$$

and the Lagrangians which couple vector mesons and kaons

$$\mathcal{L}_{VK\bar{K}} = g_{\rho K\bar{K}}\vec{\rho}^\mu(\bar{K}\vec{\tau}i\partial_\mu K - K\vec{\tau}i\partial_\mu \bar{K}) + (g_{\omega K\bar{K}}\omega^\mu + g_{\phi K\bar{K}}\phi^\mu)(\bar{K}i\partial_\mu K - Ki\partial_\mu \bar{K}). \tag{12}$$

The resulting electromagnetic interaction vertices are contained in the decay diagrams (a) and (b) of Figs. 4 and 5. In the local limit, the decay amplitude would be completely described by these Feynman diagrams. In contrast, the nonlocal strong interaction Lagrangians require special care in establishing gauge invariance. In doing so the charged fields are multiplied by exponentials [25] containing the electromagnetic field

$$K^\pm(y) \to e^{\mp ieI(y,x,P)}K^\pm(y) \tag{13}$$

with $I(y, x, P) = \int_x^y dz_\mu A^\mu(z)$, which gives rise to the electromagnetic gauge invariant Lagrangian

$$\mathcal{L}^{GI}_{f_0K\bar{K}} = \frac{g_{f_0K\bar{K}}}{\sqrt{2}} f_0(x) \int dy \Phi(y^2) \times \left[e^{-ieI(x+(y/2),x-(y/2),P)} K^+\left(x + \frac{y}{2}\right) \times K^-\left(x - \frac{y}{2}\right) + K^0\left(x + \frac{y}{2}\right)\bar{K}^0\left(x - \frac{y}{2}\right)\right], \tag{14}$$

with a corresponding expression for the a_0 meson. The

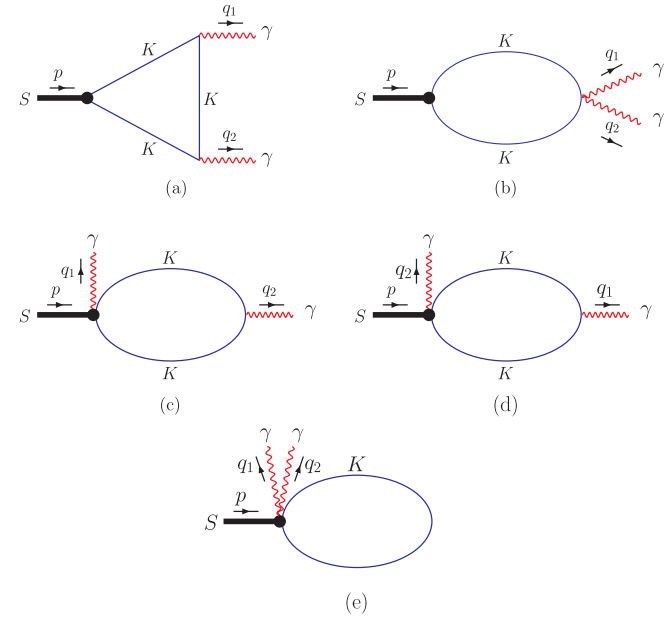

FIG. 4 (color online). Diagrams contributing to the electromagnetic $f_0 \to \gamma\gamma$ and $a_0 \to \gamma\gamma$ decays.

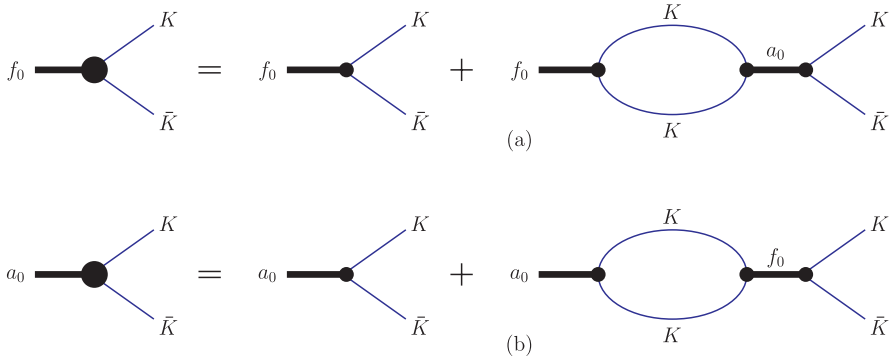

FIG. 3 (color online). Renormalization of $f_0K\bar{K}$ and $a_0K\bar{K}$ couplings due to f_0-a_0 mixing.

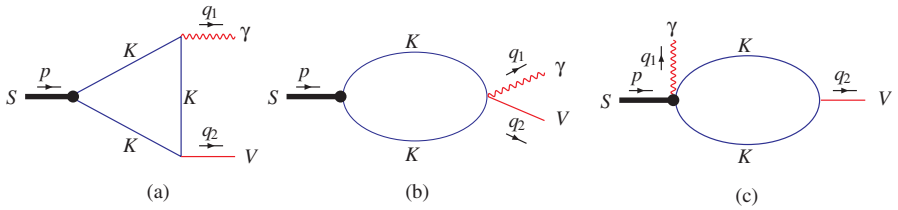

FIG. 5 (color online). Diagrams describing the $S \to \gamma V$ decays.

interaction terms up to second order in A^μ are obtained by expanding $\mathcal{L}^{GI}_{SK\bar{K}}$ in terms of $I(y, x, P)$. Diagrammatically, the higher order terms give rise to nonlocal vertices with additional photon lines attached. The Feynman rules for these vertices have been already derived in [20]. Altogether, we obtain further graphs (Fig. 4(c)–4(e)) governing the two-photon decay and the diagram of Fig. 5(c) when massive vector mesons are involved. In a slightly modified form the diagrams of Fig. 5 are also used to calculate the $\phi \to S\gamma$ decay [26–28]. Quantitatively, the decay amplitude is dominantly characterized by the triangle diagram. The Feynman graphs containing contact vertices arising due to the nonlocality only give a minor contribution to the transition amplitude but are required in order to fully restore gauge invariance.

The diagrams are evaluated by applying the technique developed in [20,21,23], where each Feynman integral is separated into a part obeying gauge invariance and a remainder term. The remainder terms of each graph cancel each other in total and only the gauge invariant structure of the decay matrix element is left. The matrix element can therefore be written by a linear combination of the form factors $F(p^2, q_1^2, q_2^2)$ and $G(p^2, q_1^2, q_2^2)$ of the respective decay

$$\mathcal{M}^{\mu\nu} = e^2(F(p^2, q_1^2, q_2^2)b^{\mu\nu} + G(p^2, q_1^2, q_2^2)c^{\mu\nu}), \quad (15)$$

where the tensor structures are given by

$$b^{\mu\nu} = g^{\mu\nu}(q_1q_2) - q_1^\mu q_2^\nu,$$
$$c^{\mu\nu} = g^{\mu\nu}q_1^2q_2^2 + q_1^\mu q_2^\nu(q_1q_2) - q_1^\mu q_1^\nu q_2^2 - q_2^\mu q_2^\nu q_1^2. \quad (16)$$

Here, p and q_1 are the four-momenta of the scalar meson and photon; q_2 is the momentum of the vector meson or second photon depending on the respective decay.

Since in the transition processes we deal with at least one real photon, the second part of $\mathcal{M}^{\mu\nu}$ proportional to $c^{\mu\nu}$ vanishes. The decay constant is therefore characterized by the form factor F which is obtained by evaluating the Feynman integrals for on-shell initial and final states, where $V = \rho, \omega, \phi, \gamma$ represents the vector particle appropriate for the respective decay. In order to allow for f_0-a_0 mixing, we use $g_{f_0K^+K^-}$ and $g_{a_0K^+K^-}$ to compute the couplings characterizing the electromagnetic decays

$$g_{S\gamma\gamma} \equiv F_{S\gamma\gamma}(M_S^2, 0, 0) = \frac{2}{(4\pi)^2} \cdot \frac{G_{SK\bar{K}}}{\sqrt{2}} I_{S\gamma\gamma}(M_S^2, 0, 0),$$
$$g_{S\gamma V} \equiv F_{S\gamma V}(M_S^2, 0, M_V^2)$$
$$= \frac{2}{(4\pi)^2} g_{VK\bar{K}} \frac{G_{SK\bar{K}}}{\sqrt{2}} I_{S\gamma V}(M_S^2, 0, M_V^2),$$
$$g_{\phi S\gamma} \equiv F_{\phi S\gamma}(M_\phi^2, M_S^2, 0)$$
$$= \frac{2}{(4\pi)^2} g_{\phi K\bar{K}} \frac{G_{SK\bar{K}}}{\sqrt{2}} I_{\phi S\gamma}(M_\phi^2, M_S^2, 0), \quad (17)$$

where I denotes the loop integrals and $G_{f_0K\bar{K}}$ and $G_{a_0K\bar{K}}$ are the dressed couplings due to f_0-a_0 mixing. The explicit expressions for the loop integrals I are given in Appendix A. The issue of gauge invariance is considered in more detail in Appendix B and in the case of the two-photon decay in [17,20]. In [17] we also considered nontrivial $K\bar{K}\gamma$ interaction vertices, where these effects are absorbed in monopole form factors $F_{K\bar{K}\gamma}(Q^2) = \frac{1}{1+Q^2/\Lambda^2_{K\bar{K}\gamma}}$ depending on the photon momentum Q^2. However, this photon form factor does not influence the decay properties when dealing with real photons as in the present considerations.

D. Strong decays

In order to calculate the strong decays of the f_0 and a_0 mesons we proceed in analogy with the computation of the $f_0 \to \pi\pi$ decay in [17]. In the present paper we extend the formalism by including the $a_0 \to \pi\eta$ decay and, additionally, by considering mixing between both scalars.

According to the interaction Lagrangians

$$\mathcal{L}_{K^*K\pi} = \frac{g_{K^*K\pi}}{\sqrt{2}} K^{*\dagger}_\mu \vec{\pi}\vec{\tau} i\overleftrightarrow{\partial}^\mu K + \text{H.c}, \quad (18)$$

$$\mathcal{L}_{K^*K\eta} = \frac{g_{K^*K\eta}}{\sqrt{2}} K^{*\dagger}_\mu \eta i\overleftrightarrow{\partial}^\mu K + \text{H.c.}, \quad (19)$$

the final-state interaction effect in the t-channel proceeds via K^* exchange (see Fig. 6(a)), where the massive vector meson is described by the antisymmetric tensor field $W_{\mu\nu} = -W_{\nu\mu}$. Therefore, the phenomenological Lagrangian which generates the contributing meson-loop diagrams is characterized by the Lagrangian

$$\mathcal{L}_W(x) = -\tfrac{1}{2}\langle \nabla^\sigma W_{\sigma\mu}\nabla_\nu W^{\nu\mu} + iG_V W_{\mu\nu}[u^\mu u^\nu]\rangle, \quad (20)$$

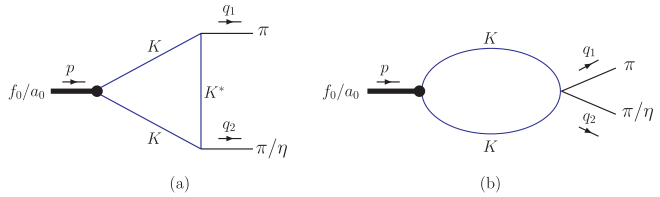

FIG. 6 (color online). Diagrams contributing to the strong decays.

which involves vector mesons in the tensorial representation [29–31]. By using low-energy theorems G_V can be expressed through the leptonic decay constant $G_V = F/\sqrt{2}$. The K^* propagators in vector representation $S^V_{K^*;\mu\nu,\alpha\beta}(x)$ and tensorial description $S^W_{K^*;\mu\nu,\alpha\beta}(x)$ differ by a term which is reflected in a second diagram containing an explicit four meson vertex (see Fig. 6(b))

$$S^W_{K^*;\mu\nu,\alpha\beta}(x) = S^V_{K^*;\mu\nu,\alpha\beta}(x) + \frac{i}{M^2_{K^*}}[g_{\mu\alpha}g_{\nu\beta} - g_{\mu\beta}g_{\nu\alpha}]\delta^4(x). \quad (21)$$

Note that we include the interaction of four pseudoscalar mesons at leading $O(p^2)$ order in the chiral expansion given by chiral perturbation theory (ChPT) [29,32]:

$$\mathcal{L}_U(x) = \frac{F^2}{4}\langle D_\mu U(x) D^\mu U^\dagger(x) + \chi U^\dagger(x) + \chi^\dagger U(x)\rangle, \quad (22)$$

which leads to the four meson $\pi\pi K\bar{K}$ interaction vertex. Inclusion of e.g. scalar resonances in the s-channel is of higher order, $O(p^4)$. In the t-channel we include the important vector meson exchange which also is of higher order, $O(p^4)$, but is important for the inclusion of final-state interactions. Here we use the standard notations of ChPT. The fields of pseudoscalar mesons are collected in the chiral matrix $U = u^2 = \exp(i\sum_i \phi_i \lambda_i/F)$ with $F = 92.4$ MeV being the leptonic decay constant and D_μ is the covariant derivative acting on the chiral field. Furthermore $\chi = 2B\mathcal{M} + \cdots$, where B is the quark vacuum condensate parameter $B = -\langle 0|\bar{u}u|0\rangle/F^2 = -\langle 0|\bar{d}d|0\rangle/F^2$ and $\mathcal{M} = \mathrm{diag}\{\hat{m}, \hat{m}, M_S\}$ is the mass matrix of current quarks with $\hat{m} = (M_u + M_d)/2$. In the leading order of the chiral expansion the masses of pions and kaons are given by $M^2_\pi = 2\hat{m}B$, $M^2_K = (\hat{m} + M_S)B$. In summary, second order ChPT gives rise to a second diagram being of the same structure as graph (b) but opposite in sign. Therefore, the triangle diagram (a) gives the dominant contribution to the decay amplitude.

The couplings for the strong decays are defined by

$$g_{f_0\pi\pi} = g_{f_0\pi^+\pi^-} = 2g_{f_0\pi^0\pi^0} = G(M^2_{f_0}, M^2_\pi, M^2_\pi), \quad (23)$$

$$g_{a_0\pi\eta} = G(M^2_{a_0}, M^2_\pi, M^2_\eta), \quad (24)$$

where, in the case of the two-pion decay, we have to consider the ratio between the charged and neutral decay modes. Here, $G(p^2, q_1^2, q_2^2)$ is the structure integral of the $f_0 \to \pi\pi$ and $a_0 \to \pi\eta$ transitions, which are conventionally split into the two terms $G^{(a)}(p^2, q_1^2, q_2^2)$ and $G^{(b)}(p^2, q_1^2, q_2^2)$. They refer to the contributions of the diagrams of Figs. 6(a) and 6(b), respectively, with

$$G(p^2, q_1^2, q_2^2) = G^{(a)}(p^2, q_1^2, q_2^2) + G^{(b)}(p^2, q_1^2, q_2^2), \quad (25)$$

where

$$G(p^2, q_1^2, q_2^2) = \frac{G_{SK\bar{K}}}{\sqrt{2}} \cdot (I(M^2_{K^\pm}, p^2, q_1^2, q_2^2) + I(M^2_{K^0}, p^2, q_1^2, q_2^2)), \quad (26)$$

and $I(M^2_K, p^2, q_1^2, q_2^2)$ denotes the contributions from the intermediate charged and neutral kaons.

The expressions for the decay widths are finally given by

$$\Gamma(f_0 \to \pi\pi) = \Gamma_{f_0\pi^+\pi^-} + \Gamma_{f_0\pi^0\pi^0} = \frac{3}{2}\Gamma_{f_0\pi^+\pi^-} = \frac{3}{32\pi}\frac{g^2_{f_0\pi\pi}}{M_{f_0}}\sqrt{1 - \frac{4M^2_\pi}{M^2_{f_0}}}, \quad (27)$$

$$\Gamma(a_0 \to \pi\eta) = \frac{1}{16\pi}\frac{g^2_{a_0\pi\eta}}{M_{a_0}}\frac{\lambda^{1/2}(M^2_{a_0}, M^2_\pi, M^2_\eta)}{M^2_{a_0}}, \quad (28)$$

with the Källen function $\lambda(x, y, z) = x^2 + y^2 + z^2 - 2xy - 2xz - 2yz$.

III. RESULTS

In this section we present our predictions for the electromagnetic and strong decay properties of the scalars f_0, a_0 and its sensitivity to finite size as well as mixing effects due to isospin violation.

For all the numerical determinations we explicitly use the charged and neutral kaon masses $M_{K^\pm} = 493.677$ MeV and $M_{K^0} = 497.648$ MeV, since we consider isospin breaking effects.

For the coupling constants between the hadronic molecules and the constituent kaons we obtain

$$\begin{aligned} \frac{G_{f_0K\bar{K};L}}{\sqrt{2}} &= 2.87 \text{ Gev (local)}, \\ \frac{G_{f_0K\bar{K}}}{\sqrt{2}} &= 3.06 \text{ Gev } (\Lambda = 1 \text{ GeV}), \\ \frac{G_{a_0K\bar{K};L}}{\sqrt{2}} &= 2.44 \text{ Gev (local)}, \\ \frac{G_{a_0K\bar{K}}}{\sqrt{2}} &= 2.55 \text{ Gev } (\Lambda = 1 \text{ GeV}), \end{aligned} \quad (29)$$

where the index L refers to the local case. For the computation of the radiative decay properties we use the vector meson masses quoted in [33]

$$M_\rho = 0.7755\ \text{GeV}, \qquad M_\omega = 0.782\,65\ \text{GeV}, \qquad M_\phi = 1.02\ \text{GeV}. \tag{30}$$

The respective $g_{VK\bar{K}}$ and $g_{\omega K\bar{K}}$ couplings are fixed using the $SU(3)$ symmetry constraint:

$$g_{\rho K\bar{K}} = g_{\omega K\bar{K}} = \frac{g_{\phi K\bar{K}}}{\sqrt{2}} = \frac{g_{\rho\pi\pi}}{2} = 3 \tag{31}$$

with $g_{\rho K\bar{K}} = 6$ extracted from data on the $\rho \to \pi^+\pi^-$ decay. Note that the $SU(3)$ value for the $g_{\phi K\bar{K}}$ coupling (4.24) is close to the one predicted by data on the $\phi \to K^+K^-$ decay. In particular, using the formula for the $\phi \to K^+K^-$ decay width

$$\Gamma(\phi \to K^+K^-) = \frac{g^2_{\phi K\bar{K}}}{48\pi} M_\phi \left(1 - \frac{4M_K^2}{M_\phi^2}\right)^{3/2} \tag{32}$$

and the central value for $\Gamma(\phi \to K^+K^-) = 2.10$ MeV we deduce $g_{\phi K\bar{K}} = 4.48$. The expressions for the electromagnetic decay widths are given by

$$\Gamma_{S\gamma\gamma} = \frac{\alpha^2\pi}{4} M_S^3 g^2_{S\gamma\gamma},$$
$$\Gamma_{S\gamma\rho/\omega} = \frac{\alpha}{8} \frac{(M_S^2 - M_\rho^2)^3}{M_S^3} g^2_{S\gamma\rho/\omega}, \tag{33}$$
$$\Gamma_{\phi S\gamma} = \frac{\alpha}{24} \frac{(M_\phi^2 - M_S^2)^3}{M_S^3} g^2_{\phi S\gamma},$$

where the coupling constants describing the radiative decays are related to the form factor F as described in (17).

Within our hadronic molecule approach we obtain for the two-photon decay width of the $f_0(980)$

$$\Gamma(f_0 \to \gamma\gamma) = 0.29(0.29)\ \text{keV (local)}, \qquad \Gamma(f_0 \to \gamma\gamma) = 0.24(0.25)\ \text{keV}\ (\Lambda = 1\ \text{GeV}). \tag{34}$$

The value in brackets refers to the corresponding value when neglecting f_0-a_0 mixing effects. The sensitivity of the $f_0 \to \gamma\gamma$ decay properties on finite size effects has been intensely studied in [17], even in the case of virtual photons, and leads to a variation of $\Gamma(f_0 \to \gamma\gamma)$ with the result

$$\Gamma(f_0 \to \gamma\gamma) = 0.21\ \text{keV}(\Lambda = 0.7\ \text{GeV}) \text{–} 0.26\ \text{keV}(\Lambda = 1.3\ \text{GeV}). \tag{35}$$

In Tables I and II we draw the comparison with data and other approaches, respectively. The $f_0 \to \gamma\gamma$ width predicted by our model matches the range of values currently deduced by the experiment.

For the two-photon decay of the a_0 meson our results lie between

$$\Gamma(a_0 \to \gamma\gamma) = 0.26(0.23)\ \text{keV (local)}, \qquad \Gamma(a_0 \to \gamma\gamma) = 0.21(0.19)\ \text{keV}\ (\Lambda = 1\ \text{GeV}), \tag{36}$$

where again results without mixing are put in parentheses. By considering in addition the f_0-a_0 mixing contributions our estimates are in good agreement with the experimental result 0.3 ± 0.1 keV of Crystal Barrel [41]. Finite size effects play a comparable role as f_0-a_0 mixing since the variation of Λ from 0.7 GeV to 1.3 GeV changes $\Gamma(a_0 \to \gamma\gamma)$ by

$$\Gamma(a_0 \to \gamma\gamma) = 0.16\ \text{keV}(\Lambda = 0.7\ \text{GeV}) - 0.21\ \text{keV}(\Lambda = 1.3\ \text{GeV}). \tag{37}$$

The decay widths obtained in other approaches are combined in Table III and show a large discrepancy even for models with the same structure assumptions.

The radiative ϕ decay widths calculated in the local limit within the framework of our formalism are given by

$$\Gamma(\phi \to f_0\gamma) = 0.63\ \text{keV}, \qquad \Gamma(\phi \to a_0\gamma) = 0.41\ \text{keV}, \tag{38}$$

where without mixing we obtain $\Gamma(\phi \to f_0\gamma) = 0.64$ keV and $\Gamma(\phi \to a_0\gamma) = 0.37$ keV.

Our result for the $\phi \to f_0\gamma$ decay overestimates the value quoted by PDG (2007) [43], where the branching ratio $\Gamma(\phi \to f_0\gamma)/\Gamma_{\text{total}} = (1.11 \pm 0.07) \times 10^{-4}$ yields $\Gamma(\phi \to f_0\gamma) = 0.44$–$0.51$ keV. In the 2008 edition of PDG [33], the ratio is increased $\Gamma(\phi \to f_0\gamma)/\Gamma_{\text{total}} = (3.22 \pm 0.19) \times 10^{-4}$ which gives 1.28–1.47 keV for the $\phi \to a_0\gamma$ decay width. However our results lie within the error bars of the CMD-2 data [44] $\Gamma(\phi \to f_0\gamma) = 0.48$–$2.00$ keV.

TABLE I. Electromagnetic decay width $f_0(980) \to \gamma\gamma$: experimental data.

Experiment	[33]	[34]	[35]	[36]
$\Gamma(f_0 \to \gamma\gamma)$ [keV]	$0.29^{+0.07}_{-0.09}$	$0.205^{+0.095+0.147}_{-0.083-0.117}$	$0.31 \pm 0.14 \pm 0.09$	$0.29 \pm 0.07 \pm 0.12$

TABLE II. Electromagnetic decay width $f_0(980) \to \gamma\gamma$: theoretical approaches.

Reference	[19]	[37]	[38]	[39]	[6]	[40]	[10]
Meson structure	$(q\bar{q})$	$(q\bar{q})$	$(q\bar{q})$	$(q\bar{q})$	$(q^2\bar{q}^2)$	(hadronic)	(hadronic)
$\Gamma(f_0 \to \gamma\gamma)$ [keV]	0.24	$0.28^{+0.09}_{-0.13}$	0.31	0.33	0.27	0.20	0.22 ± 0.07

TABLE III. Electromagnetic decay width $a_0(980) \to \gamma\gamma$: theoretical approaches.

Reference	[37]	[42]	[6]	[40]
Meson structure	$(q\bar{q})$	$(q\bar{q})$	$(q^2\bar{q}^2)$	(hadronic)
$\Gamma(a_0 \to \gamma\gamma)$ [keV]	$0.3^{+0.11}_{-0.10}$	1.5	0.27	0.78

The decay width for the $\phi \to a_0\gamma$ decay slightly overestimates the PDG (2008) average value 0.3–0.35 keV ($\Gamma(\phi \to a_0\gamma)/\Gamma_{\text{total}} = (0.76 \pm 0.06) \times 10^{-4}$) but is in agreement with the experimental data of [45] predicting 0.30–0.45 keV for $\Gamma(\phi \to a_0\gamma)$.

Because of the self-consistent determination of the $g_{a_0K\bar{K}}$ coupling constant our result in the case of the a_0 production is smaller than the width $\Gamma(\phi \to a_0\gamma)$ quoted in [11,27], but we have quite good agreement with the predictions for the ϕ production of the f_0.

For the decays involving ρ and ω mesons we predict:

$$\begin{aligned}
&\Gamma(f_0 \to \rho\gamma) = 7.93(8.09)\ \text{keV (local)} \quad \text{and} \\
&\quad 7.44(7.58)\ \text{keV}\ (\Lambda = 1\ \text{GeV}), \\
&\Gamma(f_0 \to \omega\gamma) = 7.43(7.57)\ \text{keV (local)} \quad \text{and} \\
&\quad 6.99(7.12)\ \text{keV}\ (\Lambda = 1\ \text{GeV}), \\
&\Gamma(a_0 \to \rho\gamma) = 7.94(7.18)\ \text{keV (local)} \quad \text{and} \\
&\quad 7.29(6.59)\ \text{keV}\ (\Lambda = 1\ \text{GeV}), \\
&\Gamma(a_0 \to \omega\gamma) = 7.47(6.76)\ \text{keV (local)} \quad \text{and} \\
&\quad 6.88(6.22)\ \text{keV}\ (\Lambda = 1\ \text{GeV}),
\end{aligned} \tag{39}$$

The deviations from the predicted widths of Ref. [11] for the $a_0/f_0 \to \gamma\rho/\omega$ decays arise because of different assumptions for the scalar masses and couplings. In [46] the decay width $a_0 \to \gamma\rho/\omega$ calculated within the framework of a chiral unitarity approach is larger than our result because of the additional inclusion of vector mesons in the loop diagrams.

In Appendix C our full results for the radiative decays of the neutral scalars a_0 and f_0 are collected in Table VII. In the nonlocal case we have chosen $\Lambda = 1$ GeV. For comparison we also indicate the decay properties when mixing effects are neglected. For simplicity the calculations for the ϕ decay are restricted to the local limit.

In summary, our results for the electromagnetic f_0 and a_0 decay properties are in quite good agreement with present experimental data. Therefore, the hadronic molecule approach is suitable to describe radiative f_0 and a_0 decays. However, other structure components besides the $K\bar{K}$ configuration can possibly be realized. Therefore, current data do not allow any definite and final conclusion concerning the substructure of the scalar mesons since calculations based on other approaches give similar results and even overlap with each other as demonstrated in Tables II and III.

A further step forward would be a more precise experimental determination of the decay properties but also of the f_0-a_0 mixing strength to shed light on the isospin-violating mixing mechanisms. A possible access to mixing is given by the ratio between charged and neutral a_0 meson decays since the coupling to the charged $a_0^{\pm}$ mesons is not affected by mixing.

In the numerical computations of the strong $f_0 \to \pi\pi$ and $a_0 \to \pi\eta$ decays we restrict to the charged pion mass ($M_\pi \equiv M_{\pi^\pm} 139.57$ MeV) but consider explicit kaon masses $M_{K^0} \neq M_{K^\pm}$. Assuming $\Lambda = 1$ GeV we obtain the results listed in Table VIII. Our result for the strong f_0 decay

$$\Gamma(f_0 \to \pi\pi) = 57.4\ \text{MeV}, \tag{40}$$

is consistent with the experimental data listed in Table IV.

Further theoretical predictions are indicated in Table V which, unfortunately, cover a large range of values, even for the same structure assumption. Again, the present situation for $\Gamma(f_0 \to \pi\pi)$ does not allow for a clear statement concerning the f_0 structure.

For the strong $a_0 \to \pi\eta$ decay we obtain

$$\Gamma(a_0 \to \pi\eta) = 61.0\ \text{MeV} \tag{41}$$

which also matches with the experimental results listed in Table VI. Here, the quarkonium models of [38,42] clearly deliver larger results compared to the molecular interpretation and data. In the strong decay sector f_0-a_0 mixing also generates the isospin-violating decays $f_0 \to \pi\eta$ and $a_0 \to \pi\pi$. In the context of our approach we obtain the results

TABLE IV. Strong decay width $f_0(980) \to \pi\pi$: experimental data.

Data	PDG [33]	BELLE [34]	[47]
$\Gamma(f_0 \to \pi\pi)$ [MeV]	40–100	$51.3^{+20.8+13.2}_{-17.7-3.8}$	80 ± 10

TABLE V. Strong decay width $f_0(980) \to \pi\pi$: theoretical approaches.

Reference	[19]	[48]	[49]	[38]	[50]	[51]
Meson structure	$q\bar{q}$	$q\bar{q}$	$q\bar{q}$	$q\bar{q}$	$q\bar{q}$	hadronic
$\Gamma(f_0 \to \pi\pi)$ [MeV]	20	28	52–58	53	56	18.2

TABLE VI. Strong decay width $a_0(980) \to \pi\eta$: data and theoretical approaches.

Reference	[33]	[52]	[53]	[42]	[38]
		experimental data		$q\bar{q}$	$q\bar{q}$
$\Gamma(f_0 \to \pi\pi)$ [MeV]	50–100	$50 \pm 13 \pm 4$	61 ± 19	225	138

TABLE VII. f_0 and a_0 decay properties with and without f_0-a_0 mixing for local and nonlocal ($\Lambda = 1$ GeV) interaction.

		Without mixing		With mixing	
		local	nonlocal	local	nonlocal
$f_0 \to \gamma\gamma$	g [GeV^{-1}]	0.086	0.079	0.085	0.078
	Γ [keV]	0.29	0.25	0.29	0.24
$f_0 \to \rho\gamma$	g [GeV^{-1}]	0.425	0.411	0.421	0.407
	Γ [keV]	8.09	7.58	7.93	7.44
$f_0 \to \omega\gamma$	g [GeV^{-1}]	0.431	0.418	0.427	0.414
	Γ [keV]	7.57	7.12	7.43	6.99
$\phi \to f_0\gamma$	g [GeV^{-1}]	1.97		1.95	
	Γ [keV]	0.64		0.63	
$a_0 \to \gamma\gamma$	g [GeV^{-1}]	0.076	0.069	0.080	0.073
	Γ [keV]	0.23	0.19	0.26	0.21
$a_0 \to \rho\gamma$	g [GeV^{-1}]	0.388	0.372	0.408	0.391
	Γ [keV]	7.18	6.59	7.94	7.29
$a_0 \to \omega\gamma$	g [GeV^{-1}]	0.394	0.378	0.414	0.398
	Γ [keV]	6.76	6.22	7.47	6.88
$\phi \to a_0\gamma$	g [GeV^{-1}]	1.82		1.91	
	Γ [keV]	0.37		0.41	

TABLE VIII. Strong a_0 and f_0 decay properties.

	g [GeV]	Γ [MeV]
$f_0 \to \pi\pi$	1.40	57.4
$a_0 \to \pi\eta$	2.15	61.0
$f_0 \to \pi\eta$	0.208	0.57
$a_0 \to \pi\pi$	0.234	1.59

$$\Gamma(f_0 \to \pi\eta) = 0.57 \text{ MeV}, \tag{42}$$

$$\Gamma(a_0 \to \pi\pi) = 1.59 \text{ MeV}, \tag{43}$$

which, since the processes are forbidden by isospin symmetry, are strongly suppressed compared to the dominant strong decays discussed above.

IV. SUMMARY

The present framework, where the scalars are assumed to be hadronic $K\bar{K}$ molecules, provides a straightforward and consistent determination of the decay properties, in particular, the coupling constants and decay widths. The radiative decay properties of the a_0 and f_0 mesons have been studied comprehensively within a clear and consistent model for hadronic bound states. At the same time essential criteria such as covariance and full gauge invariance with respect to the electromagnetic interaction are satisfied.

Despite that we deal with a rather simple model, it allows to study the influence of the spatial extension of the meson molecule and isospin-violating mixing. The coupling of the hadronic bound state to the constituent kaons, including f_0-a_0 mixing effects, has been determined by the compositeness condition which reduces the number of free parameters to only one, the size parameter Λ.

Our results for the electromagnetic decays ($a_0/f_0 \to \gamma\gamma$ and $\phi \to \gamma a_0/f_0$) and, in addition, the strong decay widths ($f_0 \to \pi\pi$ and $a_0 \to \pi\eta$) are analyzed with respect to f_0-a_0 mixing and finite size effects.

We come to the conclusion that the hadronic molecule interpretation is sufficient to describe both the electromagnetic and strong a_0/f_0 decays, based on the current status of experimental data. Furthermore, the f_0-a_0 mixing strength could be determined by a precise measurement of the ratio of the charged and neutral a_0 meson decays. The f_0-a_0 mixing strength could deliver new insights into the contributions being responsible for isospin-violating mixing and the meson structure issue.

ACKNOWLEDGMENTS

This work was supported by the DFG under Contracts No. FA67/31-1, No. FA67/31-2, and No. GRK683. This research is also part of the EU Integrated Infrastructure Initiative Hadronphysics project under Contract No. RII3-CT-2004-506078 and the President Grant of Russia "Scientific Schools" No. 817.2008.2.

APPENDIX A: LOOP INTEGRALS

Here we give a short presentation of the structure integrals and its evaluation relevant for the derivation of the transition form factors. For simplicity we restrict to the diagrams of Figs. 4(a) and 4(b) and 5(a) and 5(b), which do not contain contact vertices. The additional diagrams generated due to nonlocal effects are discussed in detail in [17,20]. The full structure integrals characterizing the electromagnetic decays are given by

$$\begin{aligned} I^{\mu\nu}_{S\gamma V}(M_S^2, 0, M_V^2) &= \int \frac{d^4k}{\pi^2 i} \tilde{\Phi}(-k^2) \Big((2k + p - q)^\mu (2k - q)^\nu S_K\Big(k + \frac{p}{2}\Big) S_K\Big(k - \frac{p}{2}\Big) S_K\Big(k + \frac{p}{2} - q\Big) \\ &\quad + g^{\mu\nu} S_K\Big(k + \frac{p}{2}\Big) S_K\Big(k - \frac{p}{2}\Big)\Big), \\ I^{\mu\nu}_{\phi S\gamma}(M_\phi^2, M_S^2, 0) &= \int \frac{d^4k}{\pi^2 i} \tilde{\Phi}(-k^2) \Big(\frac{(2k - q - p)^\nu (2k - q)^\mu}{S_K(k + \frac{p}{2}) S_K(k - \frac{p}{2}) S_K(k - \frac{p}{2} - q)} + \frac{g^{\mu\nu}}{S_K(k + \frac{p}{2}) S_K(k - \frac{p}{2})}\Big), \end{aligned} \tag{A1}$$

where q is the photon momentum and p of the scalar. In the case of the two-photon decay the expressions corresponding to

all the diagrams of Fig. 4 are quoted in [17]. We use the expression for the $S \to V\gamma$ decay [Eq. (A1)] as an example to demonstrate the technique for the derivation of the loop integral $I_{S\gamma V}(M_S^2, 0, M_V^2)$. In the first step we separate the gauge invariant part of the full expression $I^{\mu\nu}$ by writing

$$I^{\mu\nu}_{S\gamma V}(M_S^2, 0, M_V^2) = I_{S\gamma V}(M_S^2, 0, M_V^2) b^{\mu\nu} + I^{(2)}_{S\gamma V}(M_S^2, 0, M_V^2) c^{\mu\nu} + \delta I_{S\gamma V}, \tag{A2}$$

where the remainder term $\delta I_{S\gamma V}$ contains the noninvariant terms. The tensor structures $b^{\mu\nu}$ and $c^{\mu\nu}$ have already been defined in (16). Since we deal with real photons, only the first term of (A2), proportional to $b^{\mu\nu}$, is relevant. In the second step Feynman parametrization is introduced and the integration over the four-momentum k is performed. For instance, in the local limit we obtain

$$I_{S\gamma V}(M_S^2, 0, M_V) = \int_0^1 d^3\alpha\, \delta\Big(1 - \sum_i \alpha_i\Big) \times \frac{4\alpha_1\alpha_3}{M_K^2 - M_S^2\alpha_1\alpha_3 - M_V^2\alpha_2\alpha_3}. \tag{A3}$$

The mathematical treatment of the diagrams including contact vertices is straightforward and in complete analogy with the above example.

The loop integrals of the diagrams contributing to the strong decays (Fig. 6(a) and 6(b)) read as

$$I^{(a)}(M_K^2, p^2, q_1^2, q_2^2) = \frac{g_\pi g_{\pi(\eta)}}{(4\pi)^2} \int \frac{d^4k}{\pi^2 i} \tilde{\Phi}(-k^2) \Big(k - \frac{p}{2} - q_2\Big)_\mu \Big(k + \frac{p}{2} + q_1\Big)_\nu S_K\Big(k + \frac{p}{2}\Big) S_K\Big(k - \frac{p}{2}\Big) S^{\mu\nu}_{K^*}\Big(k + \frac{p}{2} - q_1\Big),$$
$$I^{(b)}(M_K^2, p^2, q_1^2, q_2^2) = -\frac{1}{M_{K^*}^2} \frac{g_\pi g_{\pi(\eta)}}{(4\pi)^2} \int \frac{d^4k}{\pi^2 i} \tilde{\Phi}(-k^2) \Big(k - \frac{p}{2} - q_2\Big)\Big(k + \frac{p}{2} + q_1\Big) S_K\Big(k + \frac{p}{2}\Big) S_K\Big(k - \frac{p}{2}\Big). \tag{A4}$$

Again, we evaluate the above expressions by introducing Feynman parameters and integrating over the loop momentum k.

APPENDIX B: GAUGE INVARIANCE

In this appendix gauge invariance is demonstrated by means of the charged a_0 meson decays. The kaon-loop integral corresponding to the diagrams (a) and (b) of Fig. 5 is given by

$$I^{\mu\nu}_{\triangle} = \int \frac{d^4k}{\pi^2 i} \tilde{\Phi}(-k^2) \Big\{ S\Big(k + \frac{p}{2}\Big) S\Big(k - \frac{q}{2}\Big) S\Big(k - \frac{p}{2}\Big) \times (2k + q_2)^\mu (2k - q_1)^\nu + g^{\mu\nu} S\Big(k + \frac{p}{2}\Big) S\Big(k - \frac{p}{2}\Big) \Big\}, \tag{B1}$$

where $q = q_1 - q_2$. The part $I^{\mu\nu}_{\triangle\perp}$ being gauge invariant with respect to the photon momentum q_1^μ is separated from the so-called remainder term $\delta I^{\mu\nu}_{\triangle}$ by using

$$(2k + q_2)^\mu = (2k + q_2)^\mu_{\perp q_1} + q_1(2k + q_2)\frac{q_1^\mu}{q_1^2}, \qquad g^{\mu\nu} = g^{\mu\nu}_{\perp q_1} + \frac{q_1^\mu q_1^\nu}{q_1^2}. \tag{B2}$$

Therefore, the noninvariant term is given by

$$\delta I^{\mu\nu}_{\triangle} = \int \frac{d^4k}{\pi^2 i} \tilde{\Phi}(-k^2) \Big\{ \Big[S\Big(k + \frac{p}{2}\Big) S\Big(k - \frac{p}{2}\Big) - S\Big(k - \frac{p}{2}\Big) S\Big(k - \frac{q}{2}\Big) \Big] \frac{q_1^\mu}{q_1^2} (2k - q_1)^\nu + S\Big(k + \frac{p}{2}\Big) S\Big(k - \frac{p}{2}\Big) \frac{q_1^\mu q_1^\nu}{q_1^2} \Big\} = -\int \frac{d^4k}{\pi^2 i} \tilde{\Phi}(-k^2) S\Big(k - \frac{p}{2}\Big) S\Big(k - \frac{q}{2}\Big) \Big] \frac{q_1^\mu}{q_1^2} (2k - q_1)^\nu. \tag{B3}$$

For the bubble diagram (c) of Fig. 5 the loop integral reads as (see [20])

$$I^{\mu\nu}_{bub} = -\int \frac{d^4k}{\pi^2 i} \Big(2k + \frac{q_1}{2}\Big)^\mu k^\nu \times \int_0^1 dt \tilde{\Phi}'\Big[-\Big(k + \frac{q_1}{2}\Big)^2 t - k^2(1 - t)\Big]. \tag{B4}$$

This leads to the remainder

$$\delta I^{\mu\nu}_{bub} = \int \frac{d^4k}{\pi^2 i} \tilde{\Phi}(-k^2) \frac{q_1^\mu}{q_1^2} (2k - q_1)^\nu S\Big(k - \frac{p}{2}\Big) S\Big(k - \frac{q}{2}\Big) \tag{B5}$$

which cancels with $\delta I^{\mu\nu}_{\Delta}$ and therefore

$$\delta I^{\mu\nu} = \delta I^{\mu\nu}_{\Delta} + \delta I^{\mu\nu}_{bub} = 0. \tag{B6}$$

APPENDIX C: SUMMARY TABLE

For completeness we indicate in the following tables (VII and VIII) the full list of couplings and transition widths for electromagnetic and strong decays.

[1] N. A. Tornqvist, Z. Phys. C **68**, 647 (1995).
[2] E. van Beveren and G. Rupp, Eur. Phys. J. C **10**, 469 (1999).
[3] F. Giacosa, arXiv:0804.3216; Phys. Rev. D **75**, 054007 (2007).
[4] F. Giacosa, Phys. Rev. D **74**, 014028 (2006).
[5] R. L. Jaffe, Phys. Rev. D **15**, 267 (1977).
[6] N. N. Achasov, S. A. Devyanin, and G. N. Shestakov, Phys. Lett. B **108**, 134 (1982); **108**, 435(E) (1982).
[7] D. Black, M. Harada, and J. Schechter, Prog. Theor. Phys. Suppl. **168**, 173 (2007).
[8] A. H. Fariborz, R. Jora, and J. Schechter, Phys. Rev. D **76**, 014011 (2007).
[9] J. D. Weinstein and N. Isgur, Phys. Rev. Lett. **48**, 659 (1982); Phys. Rev. D **27**, 588 (1983); **41**, 2236 (1990).
[10] C. Hanhart, Yu. S. Kalashnikova, A. E. Kudryavtsev, and A. V. Nefediev, Phys. Rev. D **75**, 074015 (2007).
[11] Yu. Kalashnikova, A. E. Kudryavtsev, A. V. Nefediev, J. Haidenbauer, and C. Hanhart, Phys. Rev. C **73**, 045203 (2006).
[12] N. N. Achasov, S. A. Devyanin, and G. N. Shestakov, Phys. Lett. B **88**, 367 (1979).
[13] F. E. Close and A. Kirk, Phys. Lett. B **489**, 24 (2000).
[14] N. N. Achasov and A. V. Kiselev, Phys. Lett. B **534**, 83 (2002); N. N. Achasov and G. N. Shestakov, Phys. Rev. D **70**, 074015 (2004).
[15] C. Hanhart, B. Kubis, and J. R. Pelaez, Phys. Rev. D **76**, 074028 (2007).
[16] J. J. Wu, Q. Zhao, and B. S. Zou, Phys. Rev. D **75**, 114012 (2007).
[17] T. Branz, T. Gutsche, and V. E. Lyubovitskij, Eur. Phys. J. A **37**, 303 (2008).
[18] S. Weinberg, Phys. Rev. **130**, 776 (1963); A. Salam, Nuovo Cimento **25**, 224 (1962); K. Hayashi, M. Hirayama, T. Muta, N. Seto, and T. Shirafuji, Fortschr. Phys. **15**, 625 (1967).
[19] G. V. Efimov and M. A. Ivanov, *The Quark Confinement Model of Hadrons* (IOP Publishing, Bristol & Philadelphia, 1993).
[20] A. Faessler, T. Gutsche, M. A. Ivanov, V. E. Lyubovitskij, and P. Wang, Phys. Rev. D **68**, 014011 (2003).
[21] A. Faessler, T. Gutsche, V. E. Lyubovitskij, and Y. L. Ma, Phys. Rev. D **76**, 014005 (2007); A. Faessler, T. Gutsche, V. E. Lyubovitskij, and Y. L. Ma, Phys. Rev. D **76**, 114008 (2007); Phys. Rev. D **77**, 114013 (2008); Y. B. Dong, A. Faessler, T. Gutsche, and V. E. Lyubovitskij, Phys. Rev. D **77**, 094013 (2008); A. Faessler, T. Gutsche, V. E. Lyubovitskij, and Y. L. Ma, Phys. Rev. D **76**, 114008 (2007); A. Faessler, T. Gutsche, S. Kovalenko, and V. E. Lyubovitskij, Phys. Rev. D **76**, 014003 (2007).
[22] I. V. Anikin, M. A. Ivanov, N. B. Kulimanova, and V. E. Lyubovitskij, Z. Phys. C **65**, 681 (1995); M. A. Ivanov, M. P. Locher, and V. E. Lyubovitskij, Few-Body Syst. **21**, 131 (1996); M. A. Ivanov, V. E. Lyubovitskij, J. G. Körner, and P. Kroll, Phys. Rev. D **56**, 348 (1997).
[23] A. Faessler, T. Gutsche, M. A. Ivanov, J. G. Körner, and V. E. Lyubovitskij, Phys. Lett. B **518**, 55 (2001); A. Faessler, T. Gutsche, M. A. Ivanov, J. G. Korner, V. E. Lyubovitskij, D. Nicmorus, and K. Pumsa-ard, Phys. Rev. D **73**, 094013 (2006); A. Faessler, T. Gutsche, B. R. Holstein, V. E. Lyubovitskij, D. Nicmorus, and K. Pumsa-ard, Phys. Rev. D **74**, 074010 (2006).
[24] V. Baru, J. Haidenbauer, C. Hanhart, Yu. Kalashnikova, and A. E. Kudryavtsev, Phys. Lett. B **586**, 53 (2004).
[25] J. Terning, Phys. Rev. D **44**, 887 (1991).
[26] Yu. S. Kalashnikova, A. E. Kudryavtsev, A. V. Nefediev, C. Hanhart, and J. Haidenbauer, Eur. Phys. J. A **24**, 437 (2005).
[27] F. E. Close, N. Isgur, and S. Kumano, Nucl. Phys. **B389**, 513 (1993).
[28] J. A. Oller, Nucl. Phys. **A714**, 161 (2003).
[29] J. Gasser and H. Leutwyler, Ann. Phys. (N.Y.) **158**, 142 (1984).
[30] G. Ecker, J. Gasser, H. Leutwyler, A. Pich, and E. de Rafael, Phys. Lett. B **223**, 425 (1989).
[31] G. Ecker, J. Gasser, A. Pich, and E. de Rafael, Nucl. Phys. **B321**, 311 (1989).
[32] S. Weinberg, Physica A (Amsterdam) **96**, 327 (1979).
[33] C. Amsler *et al.* (Particle Data Group), Phys. Lett. B **667**, 1 (2008).
[34] T. Mori *et al.* (Belle Collaboration), Phys. Rev. D **75**, 051101 (2007).
[35] H. Marsiske *et al.* (Crystal Ball Collaboration), Phys. Rev. D **41**, 3324 (1990).
[36] J. Boyer *et al.*, Phys. Rev. D **42**, 1350 (1990).
[37] A. V. Anisovich, V. V. Anisovich, and V. A. Nikonov, Eur. Phys. J. A **12**, 103 (2001).
[38] M. D. Scadron, G. Rupp, F. Kleefeld, and E. van Beveren, Phys. Rev. D **69**, 014010 (2004); **69**, 059901(E) (2004).
[39] M. Schumacher, Eur. Phys. J. A **30**, 413 (2006); **32**, 121 (E) (2007).
[40] J. A. Oller and E. Oset, Nucl. Phys. **A629**, 739 (1998).
[41] C. Amsler, Rev. Mod. Phys. **70**, 1293 (1998).
[42] T. Barnes, Phys. Lett. B **165**, 434 (1985).
[43] W. M. Yao *et al.* (Particle Data Group), J. Phys. G **33**, 1 (2006).
[44] R. R. Akhmetshin *et al.* (CMD-2 Collaboration), Phys. Lett. B **462**, 380 (1999).
[45] M. N. Achasov *et al.*, Phys. Lett. B **479**, 53 (2000).
[46] H. Nagahiro, L. Roca, and E. Oset, Eur. Phys. J. A **36**, 73 (2008).
[47] D. Barberis *et al.* (WA102 Collaboration), Phys. Lett. B **453**, 316 (1999).
[48] M. K. Volkov and V. L. Yudichev, Yad. Fiz. **64**, 2091 (2001) [Phys. At. Nucl. **64**, 2006 (2001)].
[49] V. V. Anisovich and A. V. Sarantsev, Eur. Phys. J. A **16**, 229 (2003).
[50] L. S. Celenza, S. f. Gao, B. Huang, H. Wang, and C. M. Shakin, Phys. Rev. C **61**, 035201 (2000).
[51] J. A. Oller, E. Oset, and J. R. Pelaez, Phys. Rev. D **59**, 074001 (1999); **60**, 099906(E) (1999); **75**, 099903(E) (2007).
[52] P. Achard *et al.* (L3 Collaboration), Phys. Lett. B **526**, 269 (2002).
[53] D. Barberis *et al.* (WA102 Collaboration), Phys. Lett. B **488**, 225 (2000).